PORTIONS OF THIS DOCUMENT ARE ILLEGIBLE

LA-UR-81-2742

MASTER

TITLE CRITERIA AND TECHNIQUES FOR THREE-DIMENSIONAL TREATMENT PLANNING WITH PIONS

AUTHOR(S) Peter Berardo, Sandra Zink, Michael Paciotti, and James Bradbury

SUBMITTED TO Proceedings of the International Workshop on Pion and Heavy Ion Radiotherapy: Preclinical and Clinical Studies, Vancouver, B.C. July 1981.

Los Alamos Los Alamos National Laboratory
Los Alamos, New Mexico 87545

CRITERIA AND TECHNIQUES FOR THREE-DIMENSIONAL TREATMENT PLANNING WITH PIONS

PETER BERTING, SANDRA ZINN, MICHAEL PACIOTTI AND JAMES BRADBURY
Los Alamos National Laboratory, MS P09, Los Alamos, New Mexico 87545 USA

INTRODUCTION

The ability to predict a pion dose distribution in a patient is a major objective of the clinical trials at LAMPF. Accurate predictions are essential for evaluation of pion therapy. But accuracy must be in the context of clinical utility. That is, reasonable approximations must be made in calculational methods so that treatment planning can proceed in a timely and efficient manner. We present here a few of the techniques and current developments used to achieve that objective.

METHOD OF DOSE CALCULATION

The treatment planning program PIPLAN calculates a dose distribution by summing the contributions of individual pencil beams as they pass through various clinical appliances and patient anatomy. One-dimensional depth dose distributions for pencil beams of each type of incident particle and for each of their dose components are precalculated analytically in water and include the effects of inflight interactions, straggling, and decay. Additionally, a two-dimensional distribution is precalculated for long range neutrons that are emitted by inflight and stopping pion interactions. Secondary muons from pion decay are treated as a composite pseudo-particle with its own dose distribution. Primary electron dose is obtained from fits to high-energy electron depth-dose curves. Low-energy electron dose from muon decay is obtained from a separate model during the dose accumulation process.

For a given pencil beam, dose is distributed in depth as a function of water-equivalent range along the incident trajectory and then further distributed radially as a function of multiple Coulomb scattering. A dose calculation then entails accumulating at each point of interest the amount of energy from each incident pencil beam and then dividing by the local mass density. To model the complex, non-analytic, phase space of treatment beams, measurements of individual trajectories or rays are used as input to the

calculation. This introduces a Monte Carlo aspect into the calculation and associated statistical uncertainties. However, the otherwise analytic nature of the calculation and distributed dose for each pencil beam yields a result comparable to Monte Carlo in much less time.

Figure 1 compares the PIPLAN calculation with measurements for a medium energy, broad beam with a fixed range-shifter thickness. To date, the accuracy of the physics models is such that slight adjustments must be made in a few parameter values to achieve this degree of agreement. However, such adjustments are within the experimental uncertainties of such fundamental parameters as total energy released in star secondaries, the momentum spread of the incident beam, and the beam phase space. In fact, our current inability to measure the entire phase space of the beam passing through the primary monitor chamber used for experiments and treatments requires that normalized comparisons be made. Figure 2 shows similar results for an R-cm spread peak.

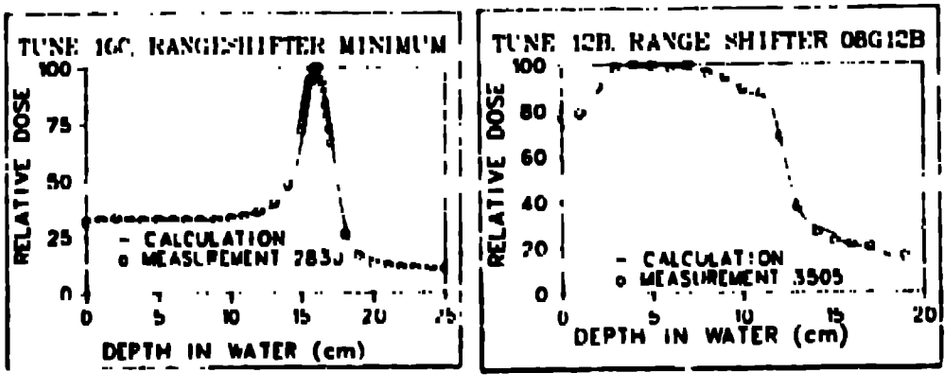

Fig. 1. Comparison of calculation and measurement of depth-dose curves for an unmodulated, medium-energy, large-field beam.

Fig. 2. Comparison of calculation and measurement of depth-dose curves for a modulated, low-energy, medium-field beam.

CT Data

The value of CT data in radiotherapy in general is widely accepted. In particular, it is used for at least three different purposes, diagnosis, treatment planning calculations, and evaluation of dose distributions on a CT image background. When different computers and hardware devices are used for these different purposes, it is possible to significantly reduce the bulk of CT data without significant of loss of resolution. The corresponding reduction in

processing time, data storage space, and data transfer time among computers can be substantial.

TABLE 1

RESULTS OF REDUCED CT NUMERICAL PRECISION AND SPATIAL RESOLUTION

CT#	TEST CASES	AVERAGE INTEGRAL CHANGES (mm)	AVERAGE INCREASE CHANGES (mm)
SPINE	4/8	-0.15 (0.40)	0.0 (0.05)
	-1,+1	-0.07 (0.38)	0.0 (0.08)
	both	-0.07 (0.37)	0.0 (0.08)
LUNG	4/8	0.0 (0.05)	0.0 (0.05)
	-1,+1	-0.02 (0.23)	0.0 (0.08)
	both	-0.02 (0.23)	0.0 (0.08)
MUSCLE	4/8	0.0 (0.06)	0.0 (0.06)
	-1,+1	0.0 (0.10)	0.0 (0.07)
	both	0.01 (0.10)	0.0 (0.07)

Treatment planning calculations use CT data for line integrals to transport particles or modify dose distributions based on effective ranges. Since integration is an averaging process, numerical and spatial resolution digitals of importance. Table 1 summarizes the results of a detailed study to determine practical limits for reduced CT numerical precision and spatial resolution using three different CT slices. Briefly, the procedure was to calculate integrals from top to bottom through each slice and tabulate the integrals on a centimeter grid. This was done for the three base cases with full resolution and for various test cases. The test case "4/8" indicates a rounding procedure that reduces the numerical precision to eight bits. This allows two CT pixels to be stored in one computer word. The "-1,+1" test cases indicate pixel averaging lateral to the line of integration. As shown these pixels were used in the lateral average which, when combined with the integration itself, implies about a ten by three pixel area average. Finally, the last test case uses both reduced resolution techniques. The resulting changes are shown with standard deviations in parentheses and assume a linear relation between CT numbers and stopping power. In fact, for heavy charged particles in material more dense

than water, the values will be even smaller. The average integral change is the average change between a final base case integral and a final test case integral. For the average increase change, the average is over the changes in the increase of all the integrals from one centimeter to the next in depth. Results such as these show that accurate calculations can be retained with at least a factor of eight reduction in the bulk of CT data through four pixel spatial averaging and eight bit numerical resolution.

Resolution reduction of CT image data, as opposed to CT treatment planning data, is subject to more subjective analysis. Visual comparisons of various images has led to the conclusion that four-pixel averaging and eight-bit precision also retains sufficient resolution and detail in a CT image for accurate evaluation of superimposed dose distributions.

Finally, we note that while these techniques preclude regeneration of a diagnostic quality image, they do allow random access of individual CT data elements. This means that treatment planning calculations and displays can proceed equally well at any orientation relative to the original CT slice.

MULTIPLE SCATTERING

A major objective of treatment planning calculations is the accurate prediction of transverse dose distributions as a function of depth and their dependence upon multiple scattering in external appliances and the heterogeneous anatomy of a patient. PIPLAN uses a recursive Gaussian model which is energy, material, and geometry dependent. The transverse distribution at any point is the result of folding together Gaussian distributions from multiple scattering at many points upstream. Although the angular distribution from multiple scattering in upstream regions is used to obtain the radial distribution downstream, in this model the angular and spatial distributions are uncoupled. That is, each scattering region assumes all incident particles are still parallel to the initial trajectory but are spatially distributed about it according to upstream scattering. This feature allows a very rapid recursive expression, but only works well for ideally thin scattering regions. To keep the calculation both fast and accurate, an empirical modifying function is used which effectively requires that the standard deviation of the transverse distribution from multiple scattering in a single thick target equals that obtained after many thin targets with the same total thickness. The net result is a recursive model that can leap large distances in a single cycle. The emphasis in the approach is not on absolute accuracy, but rather on clinically

useful and reliable accuracy. The degree of accuracy is illustrated for pions in Figure 3 for an unmodulated beam in water. In this calculation, the radiation-length of water, 36.1 cm, was used with a 0.5 cm step size in depth, which is about the maximum for a typical dose calculation.

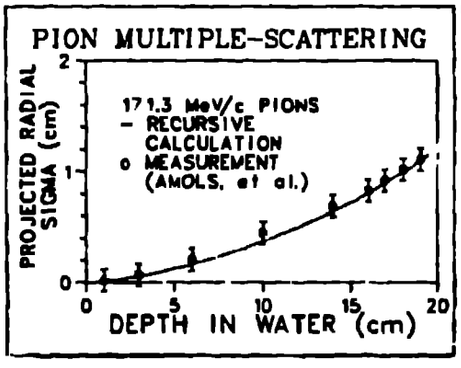

Fig. 3. Comparison of calculation and measurement of projected standard deviation for Gaussian transverse distribution as a function of depth.

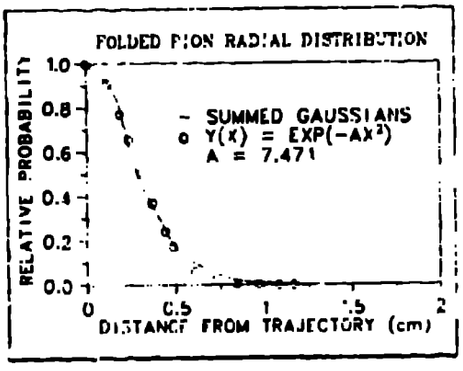

Fig. 4. Comparison of Gaussian fit to weighted and summed Gaussian transverse distributions obtained at 5 cm in water for a 4-cm range modulation and 6-cm air-gap.

When beams are range modulated, the transverse distributions at a given point due to different upstream scattering geometries must be added with weights obtained from the range modulation function. Since the sum of Gaussians is not conveniently analytic, the final transverse distribution can be obtained by tracking each ray repeatedly as a function of the range-shifter thickness or by sampling the modulation function for each ray. The first is expensive in time and the second can introduce significant statistical uncertainties in the distal spread peak unless a great number of rays are used. We are currently investigating the feasibility of tabulating for each modulation function a set of parameters at each depth along a trajectory which describe the summed distributions. We find that in most geometries a Gaussian distribution works quite well, as shown in Figure 4. For very large modulation functions, an exponential function gives only a slightly better fit than a Gaussian. If this model is successful, then the precalculated one dimensional dose distributions can be folded through the modulation function and each incident ray will distribute dose radially and in depth as if it had experienced full modulation.

PHASE SPACE SMOOTHING

Another important aspect in predicting transverse dose distributions is accurately representing the phase space of treatment beams, which at LAMPF are non-parallel and contain spatially non-uniform ratios of pions, muons, and electrons. To accurately sample and transport a sufficient number of particles in a reasonable time, two techniques are used.

The first involves measuring a dose distribution in air and also sampling the true phase space by measuring about 250,000 individual particle trajectories. Then from this phase space sample, a sub-sample is selected which reproduces the air dose distribution. The randomness of the original sample is retained in the sub-sample but the statistical uncertainty in the transverse plane is essentially reduced to that of the ion chamber, i.e., zero. The number of particles in the sub-sample is predetermined to obtain no more than a certain maximum relative statistical error in the calculations. This in turn involves the second smoothing technique.

The relative statistical error at some point in the calculation is inversely proportional to the standard deviation of the radial distribution and to the square-root of the fluence. Thus for a given relative statistical error, there is a direct relationship between the fluence in the sub-sample of particles and multiple scattering. When the fluence is also fixed, the statistical uncertainties are determined only by the degree of overlap of radial distributions. Near the surface of a patient, this overlap is small and we require a minimum radial distribution for each incident ray to achieve an overall acceptable statistical uncertainty in the entrance region. Figure 5 compares calculated transverse air scans with the ion chamber measurements for a radial sigma of 0.5 cm. This is our usual minimum sigma which means that a pencil beam is pencil-sized. At depth, the multiple scattering sigma exceeds the minimum and the statistical uncertainty is negligible, as shown in Figure 6 for a sigma of 1.7 cm. These results were obtained for a central axis fluence of only 43 particles per square centimeter. In Figure 7 are shown the transverse scans in a water phantom at mid-peak in a 10-cm spread peak and a central-axis fluence of 50 particles per square centimeter. These curves show essentially no statistical fluctuations and perhaps a small systematic coordinate misalignment.

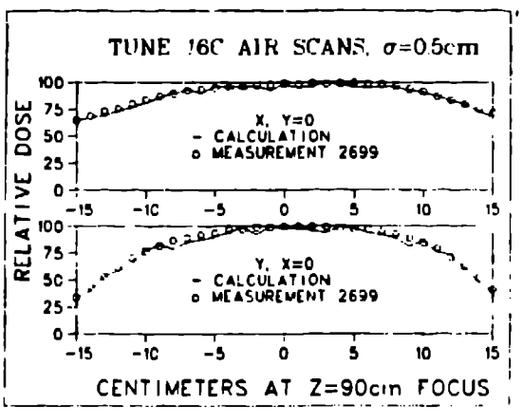

Fig. 5. Comparison of calculation and measurement of air dose on major transverse axes with minimum pencil-beam sigma.

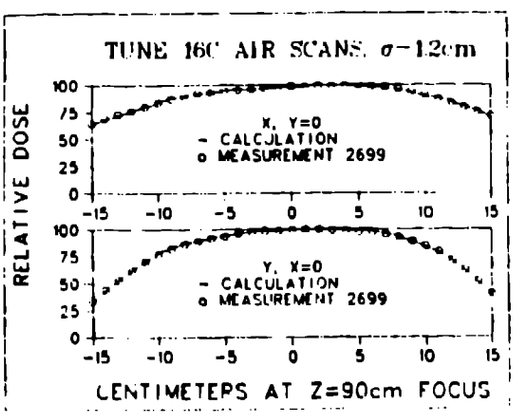

Fig. 6. Comparison of calculation and measurement of air dose on major transverse axes with typical pencil-beam sigma at depth.

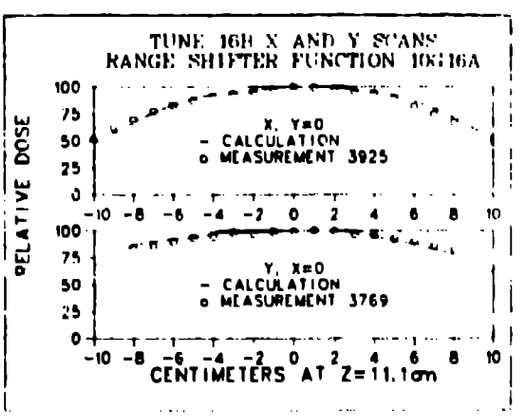

Fig. 7. Comparison of calculation and measurement of water dose on major transverse axes at depth for modulated beam.

CURRENT PROBLEMS

Collimators: The capability to predict dose distributions in complex geometries is inherent in three dimensional methods of calculation, such as Monte Carlo or three-dimensional ray tracing. This is particularly important in the regions of gross inhomogeneities, such as for a beam collimator. Here PIPLAN exhibits a problem as illustrated in Figure 8. On the left are the depth dose curves for a static rangeshifter. On the right a collimator has also been used and a clear discrepancy between calculation and measurement exists in the entrance region. Preliminary models which attempt to account for this entrance dose with neutrons from pion capture in the cerrobend collimator have not been satisfactory. As shown in Figure 9, when this beam is modulated, the discrepancy accumulates. Monte Carlo calculations are proceeding to aid our understanding of collimator physics.

Dynamic Beam Bolus: Except for strictly parallel beams and linear translation, bolus design for moving beams and/or patients presents an interesting problem, as schematically illustrated in Figure 10. In the upper left is represented the superposition of a given beam at three different focal points in a target volume, but ignoring the inhomogeneity. Each point in such a composite field can be thought of as a point source of beam particles. The points of interest are at the patient surface, as represented at the upper right. The bolus at that point must be such that the inhomogeneity is accounted for and that the optimum dose distribution is achieved in the target volume. With unlimited computer resources and time one could in principle perform iterative dose calculations to arrive at the optimum bolus and dose distribution simultaneously. In practice one must settle for something less. Using ray tracing techniques, such as exist in PIPLAN, one can determine a bolus thickness distribution for rays passing through the point in question and stopping in the target volume. This is represented in the lower left. Of course some rays may always miss the target volume and collimation or very thick bolus should be used for them, which gives the distribution on the right. The relative number of misses and target-volume stops determine if bolus or collimator is best at a given point. If bolus is used, then the bolus thickness distribution gives, to first order, the depth dose distribution under that point due to particles passing through that point. This can be used to select an actual thickness from the distribution depending upon the location of nearby critical structures or various other criteria. Since bolus itself can be very structured and act as a superficial inhomogeneity in highly non-parallel beams, it may be worthwhile to iterate at least once to refine the bolus shape. In any case, once the bolus is

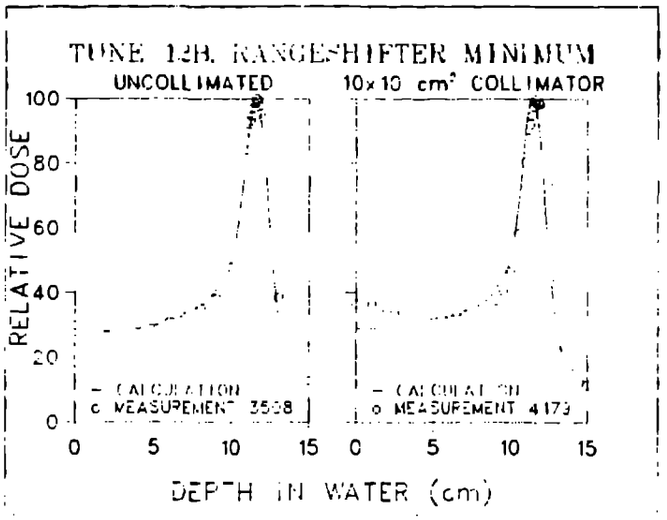

Fig. 8. Comparison of calculation and measurement of water depth-dose curves without and with collimator.

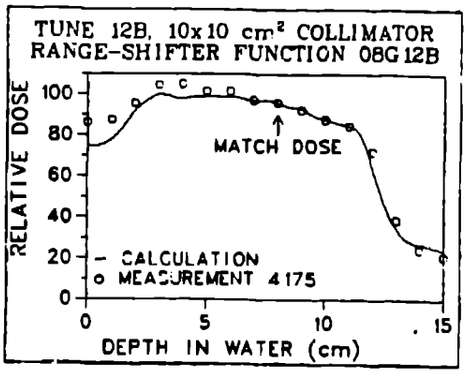

Fig. 9. Comparison of calculation and measurement of depth-dose curve for collimated and modulated low-energy, medium-field beam.

designed, calculations can proceed and results evaluated. If the dose distribution from each individual beam location is saved, then the final dose distribution can still be automatically optimized for a given bolus shape by varying the relative weights of each beam.

ACKNOWLEDGMENT

The dosimetry data used here was measured by University of New Mexico personnel under the direction of A. Smith.

REFERENCE

Amols HI et al (1981) Multiple Scattering Distributions for Therapeutic Pion Beams. Phys Med Biol 26(2): 277-289.

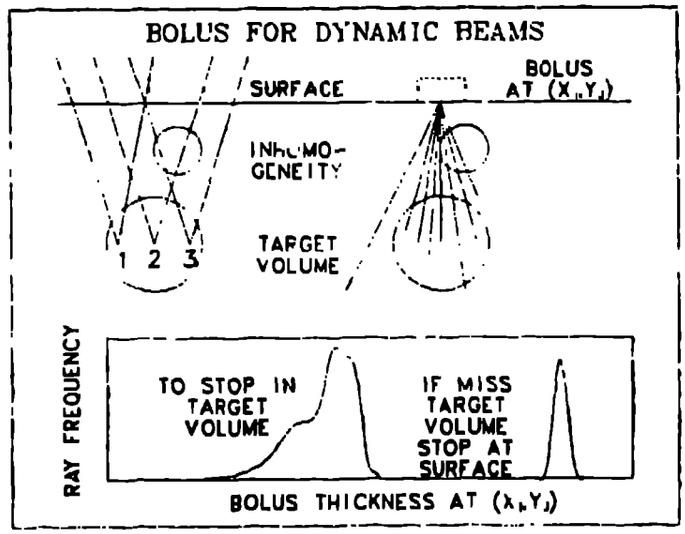

Fig. 10. For overlapping non-parallel beams, bolus-thickness distributions are obtained at each point on the patient surface. The thickness which optimizes the dose distribution is not obvious.